Scientia Iranica B (2013) 20(6), 1753–1764

SCIENTIA IRANICA

Sharif University of Technology
**Scientia Iranica**
*Transactions B: Mechanical Engineering*
www.scientiairanica.com

# Experimental and numerical investigation of radial flow compressor volute shape effects in characteristics and circumferential pressure non-uniformity

**M. Mojaddam[a], A. Hajilouy-Benisi[a,b,*] and M.R. Movahhedy[a]**

a. *School of Mechanical Engineering, Sharif University of Technology, Tehran, P.O. Box 11155-9567, Iran.*
b. *Center of Excellence for Energy Conversion, Sharif University of Technology, Tehran, P.O. Box 11155-9567, Iran.*

Received 4 August 2012; received in revised form 12 March 2013; accepted 1 July 2013

**KEYWORDS**
Radial flow compressor;
Turbocharger;
Volute;
Performance characteristic;
Pressure non-uniformity.

**Abstract.** In this article, the effects of volute cross section shape and centroid profile of a radial flow compressor volute were investigated. The performance characteristics of a turbocharger compressor were obtained experimentally by measuring rotor speed and flow parameters at the inlet and outlet of the compressor. The three-dimensional flow field model of the compressor was obtained numerically solving Navier-Stokes equations with SST turbulence model. The compressor characteristic curves were plotted. For model verification, the results were compared with experimental data, showing good agreement. Modification of a volute was performed by introducing a shape factor for volute cross section geometry. By varying this parameter, new external volutes were generated and modeled while the original volute was intermediate volute. The effect of volute cross section shape on compressor pressure ratio and isentropic efficiency at design rotational speed were investigated. Also pressure non-uniformity around compressor impeller was investigated using pressure taps around the impeller outlet to verify numerical results. This effect was considered and reported for new cases using numerical results. The results show how the shape and centroid profile of volute circumferential cross sections can influence the compressor characteristics and circumferential static pressure non-uniformity.



## 1. Introduction

Radial flow compressors have broad applications in aero-space and aviation industry, especially when continuous high pressure stream in low volumetric rate is of interest. Also this type of compressor is a better choice in meeting constraints on weight and space.

Improving compressor efficiency, having desired pressure ratio along with increasing the stable operating range are the main objectives in the design stage.

Impeller, diffuser and volute are the main components of the most radial flow compressors. The stream passing the inlet of the compressor enters the rotating impeller and energy is transferred to fluid causes increase of its angular momentum. High velocity and high pressure fluid passes through diffuser for more pressure rise. A vaned diffuser is applied for more effective diffusion. A spiral-shape volute is used for collecting and delivering the compressed gas to downstream. However, further diffusion can be achieved in the volute as well.

Many studies have been performed on impellers and diffusers to improve their performances and operating ranges, but the design and optimization of volute have only received attention last two decades[1].

Volute shape has a direct and strong influence

*. *Corresponding author. Tel.:+98 21 66165512; Fax: +98 21 660000212*
*E-mail address: hajilouy@sharif.edu (A. Hajilouy)*

on compressor performance and its stable operating range. This component causes distorted pressure fields in the upstream flow passages which can lead to aeromechanical forces acting on the impeller [2]. This force is of great importance in high pressure compressors.

In order to improve the volute design, a good understanding of the flow mechanism and recognition of its effective parameters is required. Van den Braembussche and Hande [3] and Ayder et al. [4-5] show the flow inside volute is highly three-dimensional therefore one- or two-dimensional models are unable to predict the flow pattern precisely. One- or two-dimensional models were used for reproducing and validating early experimental works [6].

Measurement technology for more accurate volute flow field studies are limited and expensive due to complicated volute geometry, strong swirl of fluid entering volute and the turbulent flow inside the volute [6]. Using CFD techniques allows for prediction of flow structure and volute performance.

Through three-dimensional modeling, the effects of many parameters on volute performance have been investigated. Ayder et al. [4-5] investigated the flow in an elliptical cross section volute experimentally and numerically at design point and off-design conditions. Hagelstein et al. [7] did the same on rectangular cross section shape volute. Ayder also concluded that a volute with an elliptic cross section is more efficient than a volute with a rectangular cross section shape [8].

Dai et al. [9] studied the effects of volute size by testing two volutes differing in axial length. They found that, although the compressor performance was affected by different designs, their configurations had no impact on the impeller performance.

Tongue area effects were investigated by Xu and Muller [1] and Xu and Amano [10]. They presented the methods for tongue geometry improvements. Volute inlet effect was investigated by Kim et al. [11] and they claimed that the key parameter for volute design is volute inlet. Qiang et al. [12] studied the influence of various volute design parameters, including area and shape of the cross-section, radial location of the cross-section, location of the volute inlet and tongue geometry, on volute overall performance and concluded that the radial location of the cross-section has the strongest influence on the performance of the volute.

In present work the effects of cross section shape and also the radial locations of cross section centriods were investigated. First, a Garrett turbocharger radial flow compressor was tested and its characteristic curves were obtained. Also the static pressures around the impeller outlet were measured for investigating the effect of the pressure non-uniformity due to volute which led to a net radial force on impeller. Then the compressor was modeled and analyzed numerically using a commercial code. Numerical results were compared with the experimental results in order to evaluate the accuracy of CFD model.

In the second step, numerical scheme is used to study the effect of volute cross section shape on performance characteristics and the static pressure distribution around the impeller of the compressor.

## 2. Design method

The main objective of a volute design procedure is to define circumferential variation of the cross-sectional area [13].

If the friction in the volute is neglected, then the design can be based on conservation of angular momentum [13-14]:

$$r_c C_c = K, \tag{1}$$

where $r_c$ is the radius of the centroid of the volute cross section and $C_c$ is flow velocity at that location and $K$ is a constant. Assuming equal flow distribution from diffuser exit circumference ($\theta = 0$ to $2\pi$), then:

$$\rho_c C_c A_c = \frac{\theta}{2\pi}\dot{m}. \tag{2}$$

The gas density can be regarded as a constant due to low Mach number, thus we can have following equation,

$$\frac{A_c}{r_c} = \frac{\dot{m}}{\rho}\frac{\theta}{2\pi K}. \tag{3}$$

Eq. (3) can be used to estimate the desired cross section area as a function of $\theta$.

Frictional effect of the volute flow causes total pressure loss, which can be estimated by the friction head loss [15].

$$dh = c_f \frac{\bar{C}^2}{2g}\frac{dL}{D_h}, \tag{4}$$

where $\bar{C}$ is the flow average velocity, $D_h$ is volute hydraulic diameter and $dL = r_c d\theta$. Numerous correlation exist for calculation of friction factor $c_f$, mostly based on the Moody chart. Eq. (4) must be integrated along volute centroid profile to obtain the total friction head loss. Having frictional head loss, the cross section areas which are calculated in Eq. (3), must increase from $A_c$ to $A'_c$. By increasing the final cross section area from $A_{\text{out}}$ to corrected area, $A'_{\text{out}}$, and using mass conservation and Bernoulli equations, other cross section areas increment are calculated accordingly [15];

$$C_{\text{out}} A_{\text{out}} = C'_{\text{out}} A'_{\text{out}}$$

$$\frac{P_{\text{out}}}{\rho g} + \frac{C_{\text{out}}^2}{2g} = \frac{P_{\text{out}}}{\rho g} + \frac{C'^2_{\text{out}}}{2g} + h. \tag{5}$$

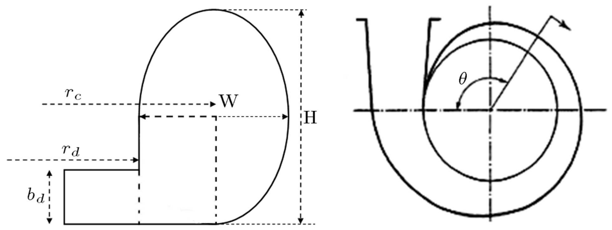


**Figure 1.** Cross section parameters (left), spiral shape and reference angle (right).

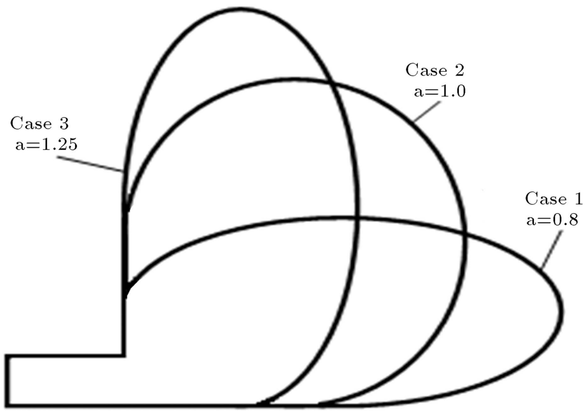


**Figure 2.** Cross section shapes of test cases.

Using Eqs. (4) and (5), outlet corrected area can be calculated as:

$$h = \frac{C_{\text{out}}^2}{2g}\left[1 - \left(\frac{A_{\text{out}}}{A'_{\text{out}}}\right)\right]. \tag{6}$$

Other circumferential area must increase by $A'_{\text{out}}/A_{\text{out}}$ ratio. In this research the cross section shape is defined by elliptical arc in three quadrants and a rectangle in the fourth quadrant, as shown in Figure 1. The centroid of this cross section placed at $r_c = r_d + 0.475W$. This geometry results in external volute, where the entire passage area is outside the diffuser exit radius.

Volute design is performed by defined cross section shape based on changing its shape factor $a$, where $H = aR$ and $W = R/a$ . Changing the shape factor affects the shape of cross section toward horizontal and vertical ellipse with constant area. Figure 2 shows the test cases which are designed for $a = 0.8, 1$ and 1.25.

The friction effect, calculated from Eqs. (3) to (5), is compensated by 10 percents increment in circumferential cross section area.

## 3. Compressor geometry

For compressor modeling, general geometry and dimensions of all components of the compressor including impeller, vane-less diffuser and volute are measured and geometric dimensions are constructed.

**Figure 3.** Tested compressor blade and geometrical models.

**Table 1.** Geometrical parameters of compressor.

| Parameter | Value |
|---|---|
| Number of blades (+ splitters) | 6(+6) |
| Blade inlet angle | 50 degree |
| Blade outlet angle | 20 degree |
| Inlet tip diameter | 58 mm |
| Inlet hub diameter | 21 mm |
| Outlet diameter | 82 mm |
| Impeller outlet width | 5.5 mm |
| Rotor axial length | 27.6 mm |
| Splitter axial length | 14.5 mm |
| Diffuser radius ratio (outlet to inlet radius) | 1.61 |

The compressor rotor and compressor casing and their geometrical models are shown in Figure 3. The main dimensions of the compressor components are tabulated in Table 1.

Having the compressor 3D model, grid generation is performed. Selection of grid type and locations for grid refinements are important in convergence of the numerical solution more rapidly.

In this simulation, unstructured tetrahedral elements were used for grid generation of stationary parts and more refinements were implemented for areas having steep gradients such as adjacent to volute tongue. Impeller grids were structured tetrahedral elements with more than 12 layers in boundary layers.

The errors which are related to the numbers of elements disappear by increasing mesh resolution. The compressor pressure ratio and efficiency at peak efficiency mass flow rate and rotational speed were taken as the parameters to compare four grid configurations to determine the influence of mesh size on the solution accuracy.

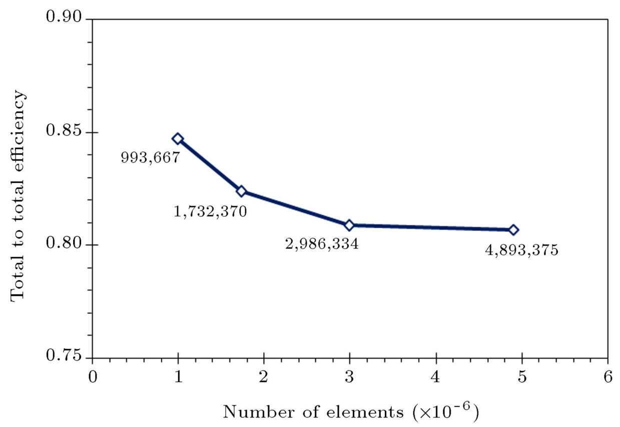


**Figure 4.** Effects of number of grids on isentropic efficiency.

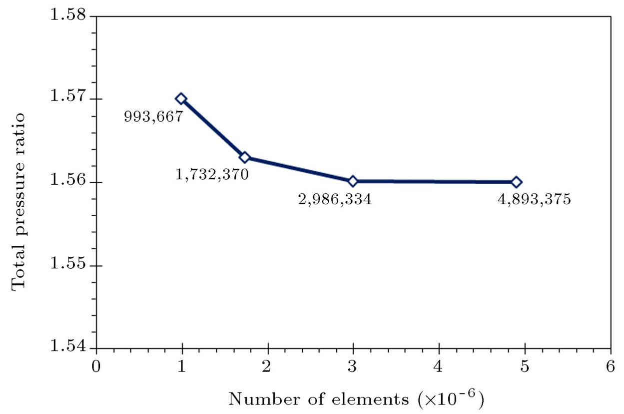


**Figure 5.** Effects of number of grids on total pressure ratio.

In Figures 4 and 5, it is observed how the compressor pressure ratio and efficiency reach an asymptotic value as the number of elements increases. According to these figures, the grid with about 1.3 million elements for stationary parts and about 280,000 elements for each passage of impeller were considered to ensure mesh independency.

## 4. Computational models

The flow field in the impeller, vane-less diffuser and volute of the compressor are analyzed, using a fully three-dimensional viscous flow modeling program. This code uses Finite Volume Method (FVM) and the Reynolds-Averaged Navier-Stokes equations (RANS) which describe the conservation of mass, momentum and energy [16].

The discretization of the equations is done via Segregated Implicit Method in which energy equation was solved independent of momentum and mass equations. The SIMPLEC algorithm is used for coupling pressure and velocity.

The Reynolds stress terms in the momentum transport equations were resolved using the Shear-Stress Transport (SST) turbulence model, developed to blend the robust and accurate formulation of the $k-\omega$ model in the near-wall region with the free-stream independence of the $k-\varepsilon$ model in the far field [17].

Using the frozen rotor method, the solution domain is divided in stationary (diffuser and volute) and rotationary (impeller) zones and utilizes relative motion between the various zones to transmit calculated values between zones via interfaces without variation of the relative position of impeller and diffuser. The interface is defined between impeller outlet and stationary part inlet [17].

Boundary conditions were set such that mass flow rate and total temperature at the inlet and averaged static pressure at the outlet were specified. Also turbulence intensity set to 5% at inlet boundary. Zero velocity or no slip conditions and no heat transfer were set for stationary walls and zero relative velocity respect to the rotating reference frame imposed for moving adiabatic walls.

Convergence criteria were considered such that the maximum residuals for mass and momentum equations were reduced to 1.0E-4.

## 5. Test facility

The turbocharger test rig at Sharif University turbocharger laboratory has been designed, established and equipped to investigate different automotive turbochargers under a variety of operation conditions based on the flow simulation of a turbocharger using compressed air [18].

The main test specifications, which can be carried out in this rig, are steady state air flow in the turbine and compressor at constant speed. The schematic arrangement of the test rig facility and test equipments are shown in Figure 6.

The turbocharger compressor absorbs the turbine output power, and controls the rotational speed of the turbocharger. The compressor takes in the air from the laboratory through air filter, orifice plate and mass flow controlling valve, which is exhausted to the atmosphere through the next controlling valve.

Five screw compressors are employed to produce high pressure air adjustable up to 13 bar gauge with 1.0 kg per sec. mass flow rate. The main compressed air supply line is a 3 inch diameter pipe, carrying the compressed and filtered air. The mass flow rate is adjusted using electro-pneumatic valves. In order to measure the steady flow air mass rate, in turbine side three flat plate orifices are used and in compressor side a bell-mouth is installed.

Static and total pressure probes are installed on inlet and outlet pipes as well as compressor casing as shown in Figures 7 and 8. Four locations are considered for measuring static pressure around impeller, also

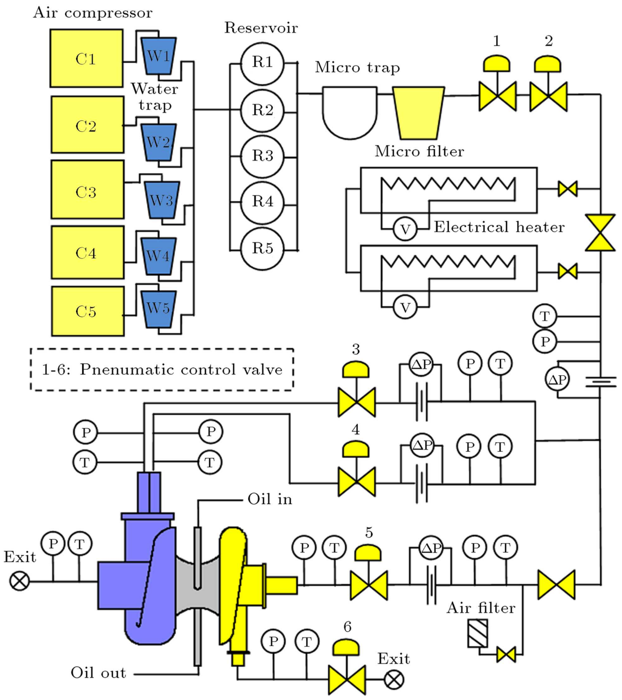


**Figure 6.** Schematic of the turbocharger test rig [19].

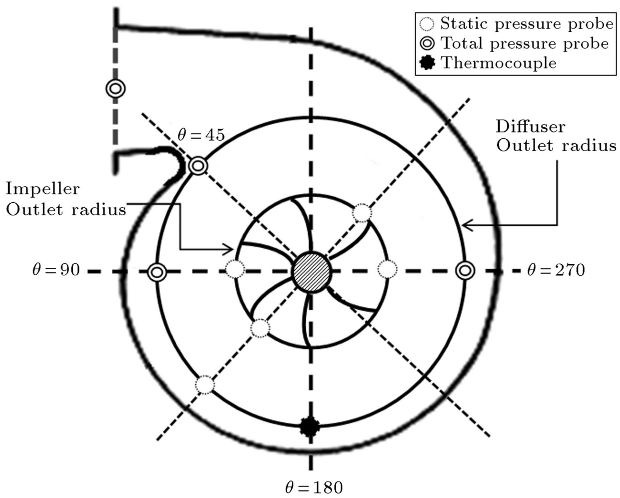


**Figure 7.** Schematic of the measurement stations on the compressor casing.

static and total pressures at volute inlet are measured to determine volute performance.

In order to measure the pressure accurately, three strain-gage pressure transducers, for different pressure ranges are used, one for high pressures up to 4.0 bar absolute, the other for lower pressures up to 2.5 bar absolute, and the third for measuring differential pressures up to 0.5 bar.

Calibrated J type thermocouples are used to measure temperatures throughout the test rig. Rotational speed of turbocharger is recorded by infrared speed pick-up. Data is acquired automatically by a data acquisition system on a PC [20].

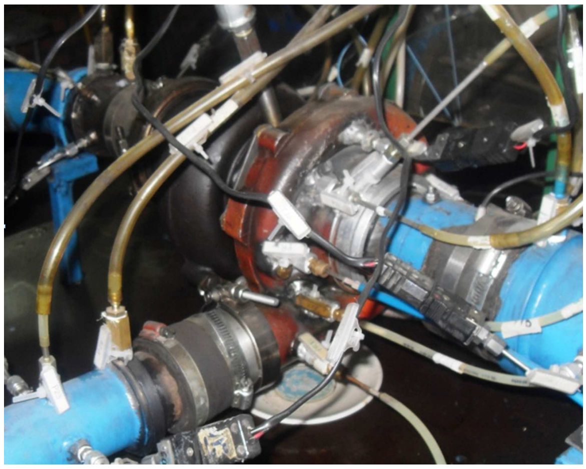

**Figure 8.** The turbocharger on test rig and measurement instruments.

## 6. Results and discussion

### *6.1. Experimental and numerical performance*

The following equations are used in obtaining the compressor characteristic curves, including total pressure ratio and efficiency versus mass parameter. Compressor total pressure ratio, calculated at constant rotational speed, is defined as:

$$\mathrm{Pr} = \frac{P_{0\,\mathrm{out}}}{P_{0\,\mathrm{in}}}. \tag{7}$$

The compressor total-to-total isentropic efficiency is defined as:

$$\eta = \frac{T_{0\,\mathrm{in}}\left(\mathrm{Pr}^{\frac{\gamma-1}{\gamma}} - 1\right)}{T_{0\,\mathrm{out}} - T_{0\,\mathrm{in}}}. \tag{8}$$

Experimental results of the compressor show that the maximum efficiency occurs at 70 KRPM at mass flow rate of 0.147 kg/s.

Figures 9 and 10 show pressure ratio and total-to-total efficiency variations versus mass parameter

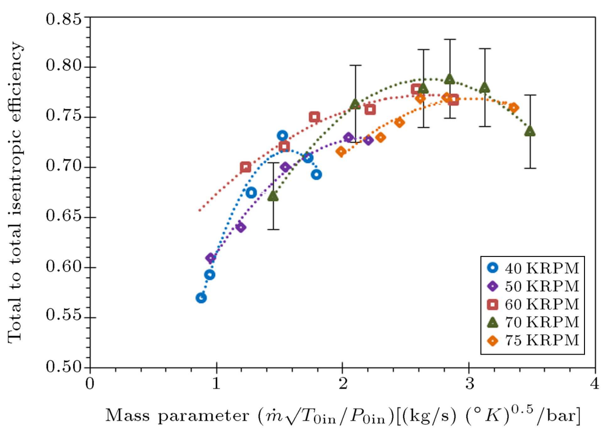


**Figure 9.** Experimental result; total to total isentropic efficiency vs. mass parameter.

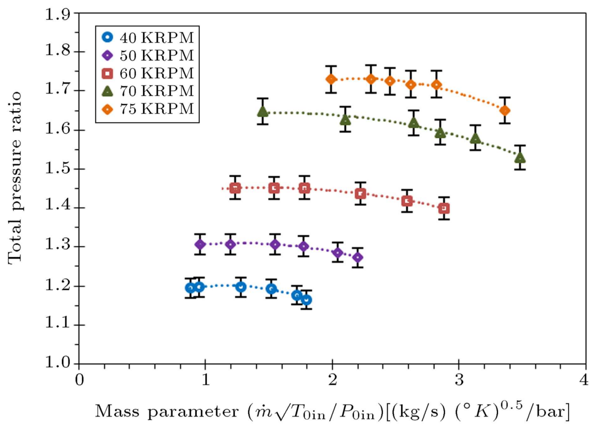


**Figure 10.** Experimental results; total pressure ratio vs. mass parameter.

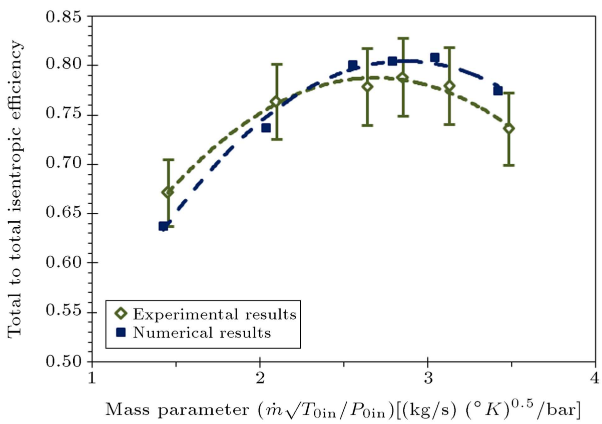


**Figure 11.** Numerical and experimental results; total to total isentropic efficiency vs. mass parameter at 70 KRPM.

for five rotational speeds, 30, 40, 50, 60, 70 and 75 KRPM. The experimental data error bars are 2 and 5 percents for total pressure ratio and total to total isentropic efficiency respectively [20]. In Figure 9, for clarity purpose, the error bars are shown only for 70 KRPM results.

Numerical results for compressor efficiency and total pressure ratio are calculated and compared with experimental results in 70 KRPM, as shown in Figures 11 and 12 respectively. In the CFD program, the boundary conditions at the inlet and outlet were derived from the experimental measurements.

Based on Figures 11 and 12, the deviations of numerical results from experimental results at 70 KRPM in maximum efficiency point are about 1.1 percent and 2.7 percent, respectively, but the differences increase in lower and higher mass flow rates up to 2.0 percent and 5.1 percent, respectively.

The differences between experimental and numerical results can be due to the following reasons:

1. The deviation of simulated model from actual geometry;

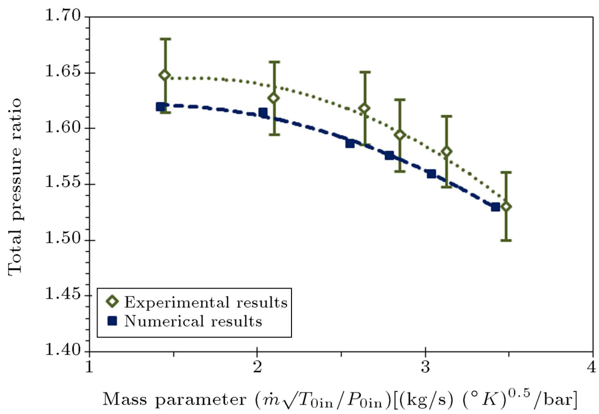


**Figure 12.** Numerical and experimental results; pressure ratio vs. mass parameter at 70 KRPM.

2. The leakages between components, heat transfer and also roughness effect that are not considered in model;
3. Existence of experimental errors in parameter measurement including systematic and random errors [18];
4. The compressor flow from impeller to the stationary components is periodic especially at off-design conditions, while the frozen rotor method is solved at steady state condition [17,21].

Also, for comparison of total to total efficiency, the uncertainty of efficiency due to pressure ratio change must be considered. Differentiating Eq. (8) with respect to pressure ratio assuming constant inlet and outlet temperatures, leads to the following relation;

$$\frac{\partial\eta}{\eta} = \frac{\gamma-1}{\gamma}\left(\frac{P_r^{\frac{\gamma-1}{\gamma}}}{P_r^{\frac{\gamma-1}{\gamma}}-1}\right)\frac{dP_r}{P_r}. \tag{9}$$

This equation shows that a one-percent change in pressure ratio (e.g. in $P_r = 1.6$) leads to 2.27 percent change in total to total efficiency in constant inlet and outlet temperatures. This analysis clarifies why the efficiency differences between experimental and numerical results are higher than the deviations in pressure ratio. Moreover, efficiency calculation is influenced by the temperature measurement errors at compressor inlet and outlet.

### 6.2. *Volute cross section shape effect*

The effect of volute profile shape on compressor performance as well as circumferential static pressure distribution is investigated by changing cross section shape while keeping the area constant. Centroid cross section profile shapes for all three cases are shown in Figure 13. As clear, the original case is an intermediate volute in which some areas of passage locate inside the diffuser exit radius.

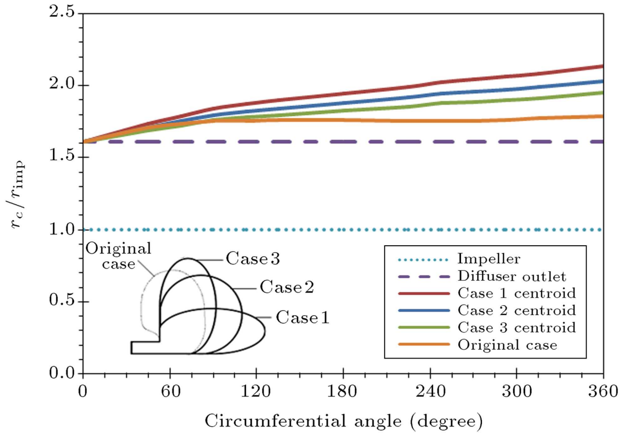


**Figure 13.** Cross section centroid profiles for all cases.

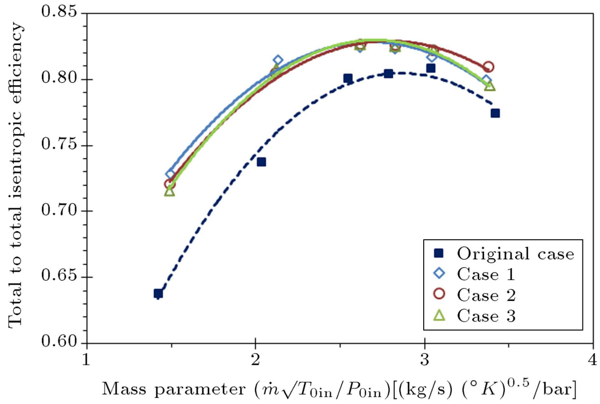


**Figure 15.** Numerical results; comparison of pressure ratio vs. mass parameter.

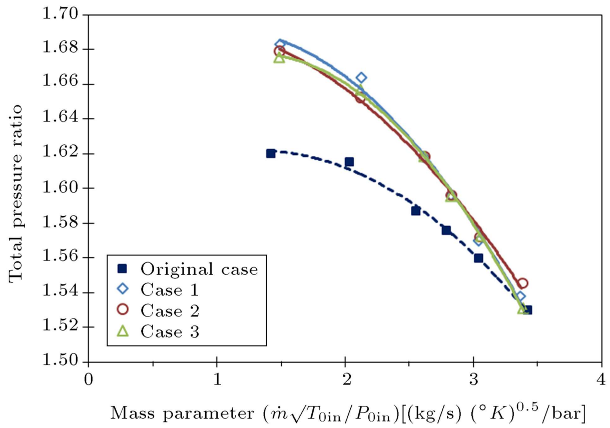


**Figure 14.** Numerical results; comparison of pressure ratio vs. mass parameter.

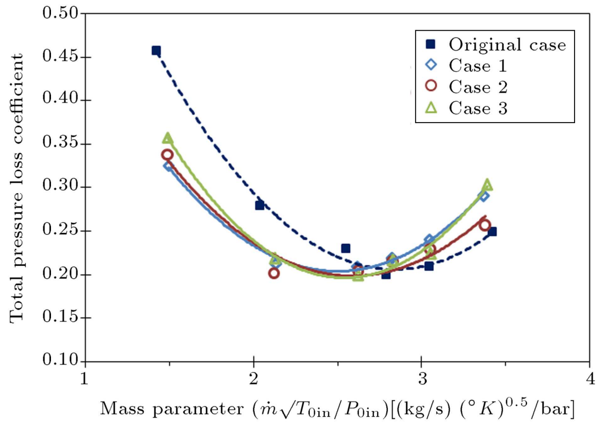


**Figure 16.** Numerical results; comparison of total pressure loss coefficients.

The considerations of grid generations and numerical solutions for new volutes were the same as the generated model described earlier. Also the same boundary conditions were applied to new models and the results were obtained. The pressure ratios were calculated using pressure mass flow average at inlet and outlet ducts.

The curves for all three cases are compared in Figure 14. This figure shows all new cases result in nearly the same values for pressure ratio and differences are limited to 0.5 percent, however the generated cases shows higher pressure ratios in compare with original case and improvement is about 1.3 percent at moderate mass flow rate and increases up to 3.9 percent in low mass flow rate at reported rotational speed.

Efficiencies of all cases are shown in Figure 15. Case 2 shows higher efficiency at high mass flow rate conditions, while case 1 has higher efficiency in low mass parameters. The highest magnitudes of efficiency for cases 1 to 3 have nearly same values and take place at the same mass flow rate. In comparison with original case, the peak efficiency of compressor is improved up to 2.7 percent. The differences between efficiencies at other mass flow rates are increased too, while as it is clear from Figure 11, the improvements are of the order of the differences between numerical and experimental results at these mass flow rates.

The overall performances of the volutes are analyzed using total pressure loss and static pressure recovery coefficients, called $K_p$ and $C_p$, respectively [14].

$$K_p = \frac{P_{0\,\text{in}} - P_{0\,\text{out}}}{P_{0\,\text{in}} - P_{\text{in}}}, \tag{10}$$

$$C_p = \frac{P_{\text{out}} - P_{\text{in}}}{P_{0\,\text{in}} - P_{\text{in}}}. \tag{11}$$

$C_p$ and $K_p$ comparison for three cases are shown in Figures 16 and 17, respectively. The original case shows higher total pressure loss and lowest static pressure recovery at low and high mass flow rates, however near the peak efficiency, all cases show almost the same coefficient values.

The reason for these differences can be explained by consideration of the flow mechanism in all cases. Previous works have reported that in the volute cross

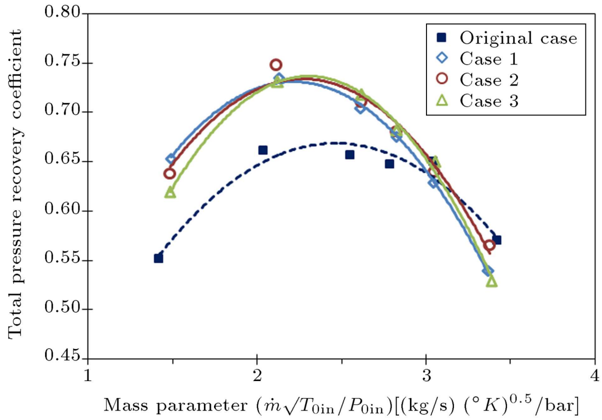


**Figure 17.** Numerical results; comparison of static pressure recovery coefficients.

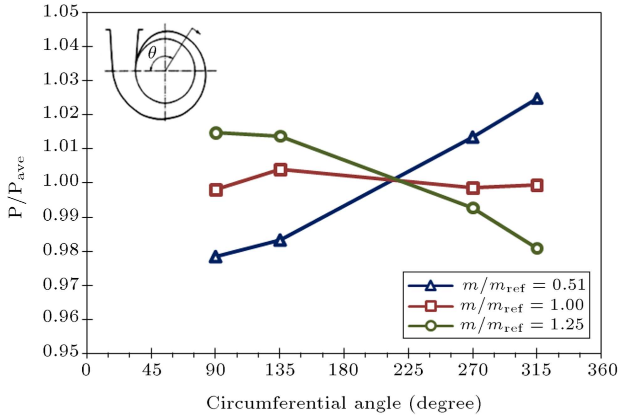


**Figure 19.** Experimental results; static pressure around impeller outlet.

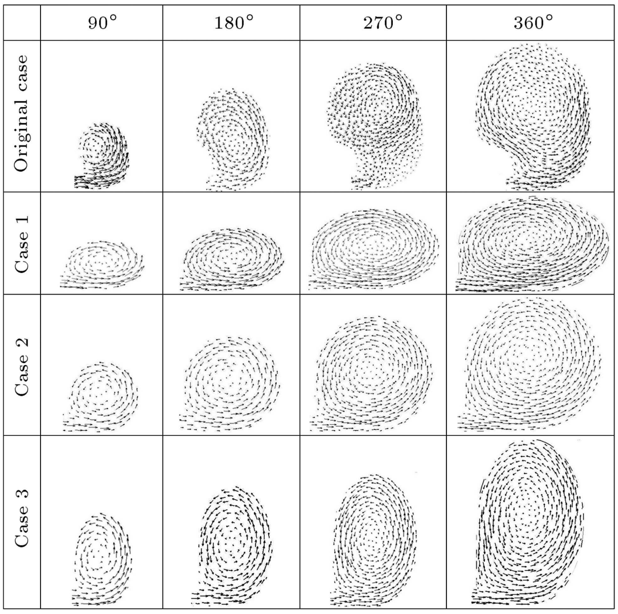


**Figure 18.** Volute cross section velocity vectors in different circumferential angles for all cases.

sections, forced vortex flow exist [4-5], which are shown in different cross sections in Figure 18.

At small circumferential angle, shear stress causes forced vortex formation, but at higher angle, the location and formation of this vortex depends on radial velocity component entered in the volute in addition to how the flow fills the volute. Moreover it depends on compressor mass flow rate and volute shape [4-5]. Referring Figure 18, for the same mass flow rate (peak efficiency point), all cross sections experience the same flow and vortex structure, but velocity vectors in external cases, cases 1 to 3, are more similar analogous trends in all cross sections. Therefore better volute performance at the same mass flow rate in these cases are expected. Also, it is seen that the flow structures in original case especially at 90 and 270 degrees circumferential angle are different from other sections due to different cross section shapes at these locations.

### *6.3. Pressure non-uniformity*

To investigate the effect of volute on circumferential pressure, the static pressures around impeller outlet are measured.

For different mass flow rates, the static pressure values are reported by dividing them to average of them at 90, 135, 270 and 315 degree circumferential angles, which are shown in Figure 19. The mass flow rates are non-dimensionalized by the reference point mass flow rate ($\dot{m}/\dot{m}_{ref}$), which has the highest efficiency in 70 KRPM rotational speed.

As it is clear, the static pressure around the impeller are increased circumferentially (from 0 degree to 360 degree) at lower mass rates and by increasing the mass flow rates to moderate values the pressure have nearly the same values around impellers. By increasing mass flow rate at constant rotational speed the circumferential static pressure are decreased around impeller.

Continuously increasing static pressure at low mass flow rate is due to the fact that the volute is oversized for low mass flow rates and acts as a difusser. Also large amount of mass flow rate causes flow acceleration and leads to pressure drop because the volute which is designed for having the highest efficiency is too small and operates as a nozzle in the circumferential direction [7].

Figure 20(a) to (c) show the numerical and experimental results for three conditions, low, moderate and high mass flow rates, respectively. The numerical results are reported at impeller outlet shroud at the same location of installed probes. The experimental results error bars for reported pressures are ±1 percent.

As it was expected, maximum pressure disturbance occurs near tongue region for all cases. The numerical results show good agreement for reported points in the range of ±1.4 precent.

Pressure non-uniformities for cases 1 to 3 are

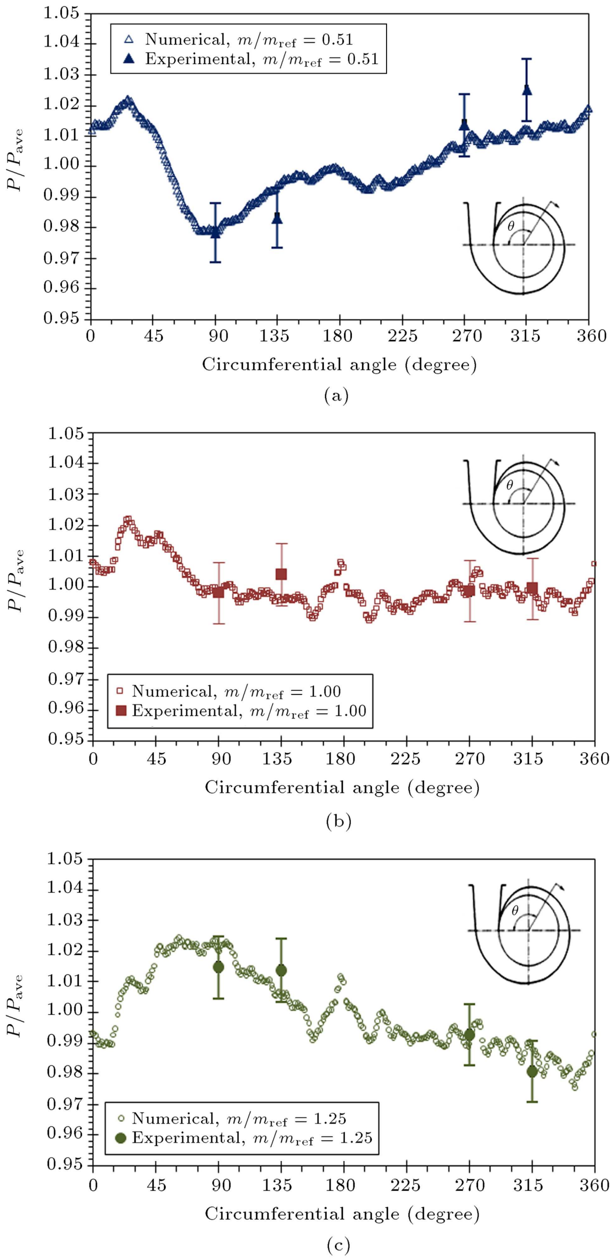


**Figure 20.** Experimental and numerical results; pressure around impeller outlet at (a) low mass flow rate, (b) moderate mass flow rate and (c) high mass flow rate.

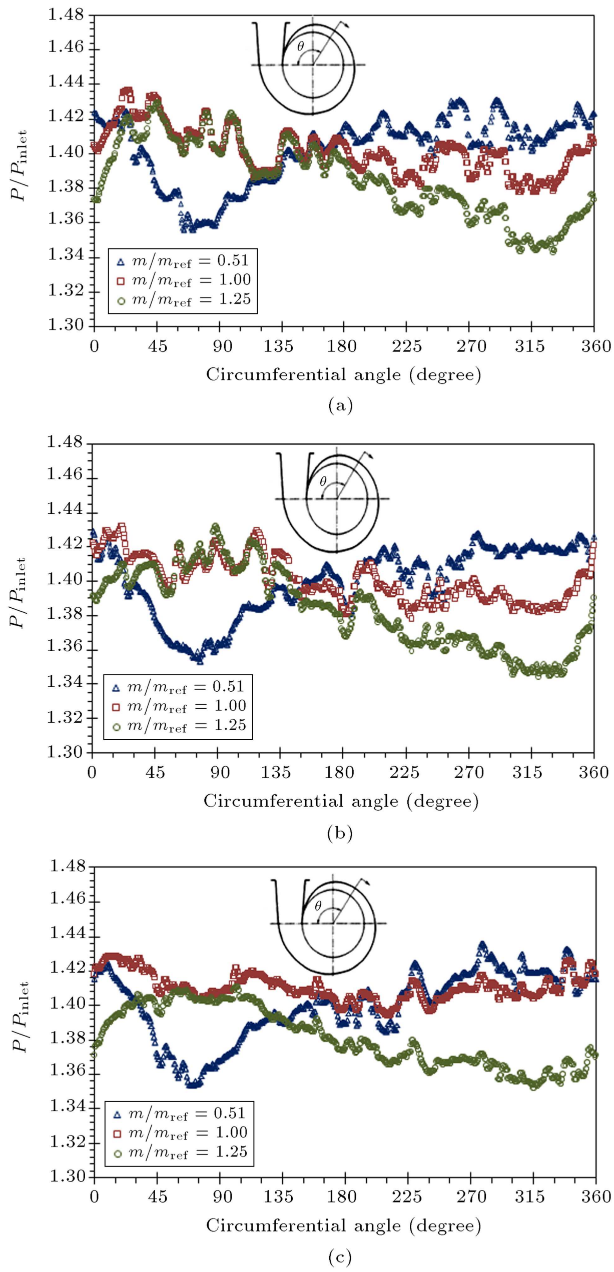


**Figure 21.** Mid line static pressure distribution at impeller outlet: (a) Case 1; (b) case 2; and (c) case 3.

shown in Figure 21(a) to (c) respectively, each one for three different mass flow rates. Pressure increasing trend around impeller for low mass rate, and decreasing trend for high mass flow rates are obvious in these figures. For recognizing the differences among these cases, the effect of these non-uniformity are considered.

Integration of static pressure at the impeller outlet gives a good approximation of the radial forces on impeller shaft for the impeller with backward-leaned blades [22]. This radial force can cause severe mechanical problem in high pressure compressor mainly at off-design conditions [2].

For integration, the circumference of impeller exit was divided in 720 equal sectors and the force for each one was calculated. The net force is a vector sum of all sector forces. The magnitude of this radial force vector is reported by using the non-dimensional radial force coefficient, $K_r$ [23].

$$K_r = \frac{F_r}{P_{0\text{out}} d_d b_d}. \tag{12}$$

The values of $K_r$ for different mass flow conditions of all cases are tabulated in Table 2, multiplying by 100.

Table 2 shows that the original case and case 3 produce less net force on impeller in reference mass

**Table 2.** Values of non-dimensional radial force coefficients ($K_r \times 100$).

| Mass flow rate | Original case | Case 1 | Case 2 | Case 3 |
|---|---|---|---|---|
| $\dot{m}/\dot{m}_{\text{ref}} = 0.51$ | 8.68 | 5.10 | 5.66 | 6.81 |
| $\dot{m}/\dot{m}_{\text{ref}} = 1.0$ | 1.69 | 3.22 | 3.71 | 1.98 |
| $\dot{m}/\dot{m}_{\text{ref}} = 1.25$ | 2.97 | 7.38 | 8.04 | 6.20 |

flow rate. In higher mass flow rate all cases show nearly the same $K_r$ except original case which shows low net force on impeller. Cases 1 and 2 have approximately the same low mass flow rate and have better conditions in comparison with other cases.

## 7. Conclusion

In this article, the effects of cross section shape of a radial flow compressor volute on its performance were investigated. A numerical model was prepared and analyzed for the compressor. Numerical results were verified through comparison with experimental data obtained from testing the radial flow compressor of a turbocharger. Experimental results included compressor characteristic curves and pressure non-uniformity around the impeller caused by volute.

Three different external volutes with constant cross section area were defined and analyzed on the same diffuser and impeller.

The results show that the external volute cases with different cross section shapes have nearly same values for compressor characteristics. However in comparison with the original case, they have higher pressure ratios and total to total isentropic efficiency.

Another factor for evaluating the effect of volute shape on compressor performance is circumferential pressure non-uniformity which causes the net radial force on impeller. Among external volutes the circular one (case 2) causes less net force on impeller in tested mass flow rates. The original volute produces the lowest net force on impeller at the reference and high mass flow rate in comparison with other cases, while it has the highest value in low mass flow rate.

## Acknowledgements

The authors gratefully acknowledge the support of research and technology office of Sharif University of technology as well as turbocharger laboratory staffs.

## Nomenclature

| | |
|---|---|
| $A$ | Volute cross section area |
| $C$ | Velocity |
| $C_p$ | Static pressure recovery coefficient |
| $D$ | Diameter |
| $D_h$ | Hydraulic diameter |
| $F$ | Radial force |
| $H$ | Volute cross section height |
| $K_P$ | Total pressure loss coefficient |
| $L$ | Circumferential length |
| $P$ | Pressure and total pressure ratio |
| $P_r$ | Total pressure ratio |
| $T$ | Temperature |
| $W$ | Volute cross section width |
| $a$ | Shape factor |
| $b$ | Diffuser width |
| $c_f$ | Friction factor |
| $d$ | Differential symbol |
| $g$ | Gravity |
| $h$ | Enthalpy |
| $\dot{m}$ | Mass flow rate |
| $r$ | Radius |

*Greek symbols*

| | |
|---|---|
| $\gamma$ | Heat capacity ratio |
| $\eta$ | Total to total isentropic efficiency |
| $\theta$ | Circumferential angle |
| $\lambda$ | Friction coefficient |
| $\rho$ | Density |

*Superscript*

| | |
|---|---|
| $'$ | Corrected value |
| $-$ | Average |

*Subscripts*

| | |
|---|---|
| 0 | Stagnation property |
| $c$ | Centroid of cross section |
| $d$ | Diffuser |
| in | Inlet |
| $m$ | Meridional component |
| out | Outlet |
| $r$ | Ratio |
| $\theta$ | Circumferential component |

## References

1. Xu, C. and Muller, M. "Development and design of a centrifugal compressor volute", *International Journal of Rotating Machinery*, **2005**(3), pp. 190-196 (2005).
2. Sorokes, J.M., Borer, C.J. and Koch, J.M. "Investigation of the circumferential static pressure non-uniformity caused by a centrifugal compressor discharge volute", *ASME*, Paper No. GT-98-326 (1998).

3. Van den Braembussche, R.A. and Hande, B. "Experimental and theoretical study of the swirling flow in centrifugal compressor volutes", *Journal of Turbomachinery*, **112**, pp. 38-43 (1990).

4. Ayder, E. and Van den Braembussche, R.A. "Numerical analysis of the three-dimensional swirling flow in centrifugal compressor volutes", *Journal of Turbomachinery*, **116**(3), pp. 462-468 (1994).

5. Ayder, E., Van den Braembussche, R.A. and Brasz, J. "Experimental and theoretical analysis of the flow in a centrifugal compressor volute", *Journal of turbomachinery*, **115**(3), pp. 582-589 (1993).

6. Zheng, Q.X., Huenteler, J., Yang, M.Y., Zhang, Y.J. and Bamba, T. "Influence of the volute on the flow in a centrifugal compressor of a high-pressure ratio turbocharger", *Proceedings of the Institution of Mechanical Engineers, Part A: Journal of Power and Energy*, **224**(8), pp. 1157-1169 (2010).

7. Hagelstein, D., Hillewaert, K., Van den Braembussche, R.A., Engeda, A., Keiper, R. and Rautenberg, M. "Experimental and numerical investigation of the flow in a centrifugal compressor volute", *Journal of turbomachinery*, **122**(1), pp. 22-31 (2000).

8. Reunanen, A. "Experimental and numerical analysis of different volutes in a centrifugal compressor", Doctoral dissertation, Lappeenranta University of Technology (2001).

9. Dai, Y., Engeda, A., Cave, M. and Di Liberti, J-L. "A flow field study of the interaction between a centrifugal compressor impeller and two different volutes", *Proceedings of the Institution of Mechanical Engineers, Part C: Journal of Mechanical Engineering Science*, **224**(2), pp. 345-356 (2010).

10. Xu, C. and Amano, R. "Eliminating static pressure distortion by a large cut back tongue volute", *ASME*, Paper No. GT2006-90001, pp. 155-164 (2006).

11. Kim, S., Park, J., Ahn, K. and Baek, J. "Improvement of the performance of a centrifugal compressor by modifying the volute inlet", *Journal of Fluids Engineering*, **132**(9), pp. 091101.1-091101.7 (2010).

12. Qiang, X., Teng, J. and Du, Z. "Influence of various volute designs on volute overall performance", *Journal of Thermal Science*, **19**(6), pp. 505-513 (2010).

13. Aungier, R.H. *Centrifugal Compressors: A Strategy for Aerodynamic Design and Analysis*, 1st Ed., pp. 196-200, ASME Press, New York, USA (2000).

14. Japikse, D. *Centrifugal Compressor Design and Performance*, 1st Ed., pp. 12-21 (Ch. 4), Concepts ETI Inc., Vermont, USA (1996).

15. Rezaei, H. "Investigation of the flow structure and loss mechanism in a centrifugal compressor volute", Doctoral Dissertation, Michigan State University (2001).

16. Shahhosseini, M., Hajilouy-Benisi, A. and Rad, M. "Numerical and experimental investigation of the flow and performance characteristics of twin-entry radial turbine under full and partial admission conditions", *ASME* Paper No. GT-2008-50397, pp. 1507-1517 (2008).

17. Nili-Ahmadabadi, M., Hajilouy-Benisi, A., Durali, M. and Ghadak, F. "Investigation of a centrifugal compressor and study of the area ratio and TIP clearance effects on performance", *Journal of Thermal Science*, **17**(4), pp. 314-323 (2008).

18. Hajilouy-Benisi, A., Rad, M. and Shahhosseini, M.R. "Flow and performance characteristic of twin-entry radial turbine under full and extreme partial admission conditions", *Archive of Applied Mechanics*, **79**(12), pp. 1127-1143 (2009).

19. Mojaddam, M., Hajilouy-Benisi, A. and Movahhedy, M.R. "Investigation on effect of centrifugal compressor volute cross-section shape on performance and flow field", *ASME TurboExpo Conference*, Copenhagen (2012).

20. Hajilouy-Benisi, A., Rad M. and Shahhosseini, M.R. "Empirical assessment of the performance characteristics in turbocharger turbine and compressor", *Experimental Techniques*, **34**(3), pp. 54-67 (2010).

21. Khalfallah, S. and Ghenaiet, A. "Analyses of impeller-vaneless-diffuser-scroll interactions in a radial compressor", *Proceedings of the Institution of Mechanical Engineers, Part A: Journal of Power and Energy*, **224**(6), pp. 851-867 (2010).

22. Fatsis, A., Pierret, S. and Van den Braembussche, R. "Three-dimensional unsteady flow and forces in centrifugal impellers with circumferential distortion of the outlet static pressure", *Journal of Turbomachinery*, **119**(1), pp. 94-102 (1997).

23. Reunanen, A. and Larjola, J. "Radial forces in a centrifugal compressor; Experimental investigation by using magnetic bearings and static pressure distribution", *Journal of Thermal Science*, **14**(1), pp. 1-8 (2005).


## Biographies

**Mohammad Mojaddam** received his BSc and MSc degrees in Mechanical Engineering at Sharif University of Technology (SUT), Tehran, Iran in 2007 and 2009, respectively. Since then he is a PhD student of Mechanical Engineering, Energy Conversion, at Mechanical Engineering Department of SUT. Working on his PhD thesis make him experienced in experimental study of turbo-machines specially turbochargers, radial flow compressors and radial turbines. His research interests are design, modeling (CFD), optimization and also measurement techniques in turbo-machinery especially in compressor components.

**Ali Hajilouy-Benisi** received his PhD degree from Mechanical Engineering Department of Imperial College at the University of London in 1993. He has been faculty member of the Institute of Water and Energy and then the School of Mechanical Engineering at Sharif University of Technology (SUT) since 1978. He served as director of the fluid mechanics lab. from 1993-1995, founder and director of the turbocharger lab. from 1993, founder and director of the turbocharging lab. from 2000, founder and director of the gas turbine lab. from 2008 at the school of mechanical engineering of SUT. He has also served as research director of the SUT from 1993-1995. His research interests are experimental and theoretical investigations of turbochargers, turbocharging, and gas turbines.

He is author or co-author of over 90 conferences and journal papers, and coordinator for compiling and publishing four volumes research reports of SUT for 1991-1995. He and one of his students are translators of an English text book to Farsi (Persian). He has also supervised over 40 graduate theses. He has conducted more than seven research funded projects.

**Mohammad Reza Movahhedy** received his BS degree from University of Tehran, Iran in 1988, his MS degree from the University of Waterloo, Canada in 1994, and his PhD degree from the University of British Columbia, Canada in 2000, all in Mechanical Engineering. He is currently professor in the Department of Mechanical Engineering at Sharif University of Technology, Iran. His research interests are FEM simulation of metal cutting/forming processes, machine tool dynamics, mechanics of machining processes, experimental modal analysis and computer aided tolerancing.